JOURNAL OF GEOPHYSICAL RESEARCH, VOL. 104, NO. C5, PAGES 11,077–11,085, MAY 15, 1999

Intrusion of the Southwest Monsoon Current into the Bay of Bengal

P. N. Vinayachandran,[1] Yukio Masumoto,[1,2] Tetsuya Mikawa,[3] and Toshio Yamagata[1,2]

Abstract. The general eastward flow in the north Indian Ocean during summer, which is called the Southwest Monsoon Current (SMC), flows eastward south of India, turns around Sri Lanka, and enters the Bay of Bengal. The intrusion of the SMC into the Bay of Bengal is studied using expendable bathythermograph (XBT) observations along the shipping route between Sri Lanka and Malaca Strait, TOPEX/POSEIDON sea surface height anomalies, and an ocean general circulation model. The intrusion appears first as a broad northward shallow (confined to the upper 200 m) flow in the central part of the Bay of Bengal during May. As the summer season advances, it moves westward, intensifies, and becomes narrow. The mean seasonal (May–September) transport of the SMC into the Bay of Bengal is about 10 Sv. The zonal variation of the geostrophic velocity across 6°N calculated using the XBT data compares well with that from TOPEX/POSEIDON altimeter data. However, the SMC in the XBT data is faster (40 cm s^{-1}) than in the altimeter data or the numerical simulation (25 cm s^{-1}). Harmonic analysis of the depth of 20°C isotherm together with a simple forced Rossby wave model demonstrates that the SMC east of Sri Lanka is forced by both Ekman pumping in the Bay of Bengal and Rossby wave radiation associated with the spring *Wyrtki* [1973] jet in the equatorial Indian Ocean. The initial intrusion of the SMC into the Bay of Bengal is attributed to this Rossby wave radiation from the eastern boundary.

1. Introduction

The monsoon winds that blow over the north Indian Ocean bring about spectacular reversal of the ocean circulation. Near the western boundary of the Indian Ocean the Somali Current flows southward during the boreal winter and northward during the summer [*Schott*, 1983]. The flow pattern elsewhere north of the equator also undergoes similar reversal. During the northeast monsoon (December–February) the surface current is westward north of the equator in response to the northeasterly winds, and it is called the Northeast Monsoon Current. During the summer monsoon (May–September) the winds are southwesterly, and the surface current is generally toward east and is called the Southwest Monsoon Current (SMC). The SMC appears as an extension of the Somali Current system in the western Arabian Sea, flows toward the southeast in the eastern Arabian Sea, and then flows eastward south of India [*Hastenrath and Greischar*, 1991]. East of Sri Lanka, a part of the SMC turns around Sri Lanka and flows into the Bay of Bengal. The surface flow east of Sri Lanka acquires speeds greater than 40 cm s^{-1} [*Hastenrath and Greischar*, 1991]. Direct current measurements south of Sri Lanka show that the transport of the SMC is in the range of 8–15 Sv (1 Sv = 10^6 m^3 s^{-1}) in July [*Schott et al.*, 1994].

[1]Institute for Global Change Research, Frontier Research System for Global Change, Tokyo.
[2]Department of Earth and Planetary Physics, Graduate School of Science, University of Tokyo, Tokyo.
[3]Climate Prediction Division, Japan Meteorological Agency, Tokyo.

Paper number 1999JC900035.
0148-0227/99/1999JC900035$09.00

The SMC is important because of its role on the interbasin exchange of water between the Arabian Sea and the Bay of Bengal. These two basins located along the same latitude are influenced by monsoons and feature a seasonal warm pool [*Vinayachandran and Shetye*, 1991]. However, they show large differences in their salinity because of the excess evaporation over the Arabian Sea in contrast to the large freshwater input into the Bay of Bengal. It is not understood yet how the two basins exchange fresh water (salt) and heat. Currents along the west and east coasts of India [*Shetye et al.*, 1991, 1996] suggest a possible link between these two basins via the coastal circulation girdling India and Sri Lanka. Recent direct current measurements south of Sri Lanka [*Schott et al.*, 1994] suggest that the circulation along the coast of Sri Lanka could be an important link that connects the coastal currents along the east and west coasts of India, supporting the above argument. Recent model results [*Vinayachandran and Yamagata*, 1998] (hereafter referred to as VY98) also suggest the existence of an open ocean link connecting the two basins through the SMC. Observations south of India and around Sri Lanka that are needed to establish the water pathway are still very poor.

Intrusion of the SMC into the Bay of Bengal is well manifested in climatological data sets (Figure 1). Ship drifts [*Cutler and Swallow*, 1984] show that major part of the SMC curves around Sri Lanka to flow into the Bay of Bengal, while the rest continues eastward. Geostrophic currents calculated from temperature and salinity climatologies [*Levitus and Boyer*, 1994; *Levitus et al.*, 1994] also show the intrusion. However, in contrast to the ship drifts, the branch that flows into the bay is fed by a westward flow originating farther to the east. Although climatological data sets reveal the path of the SMC into the bay, flow characteristics east of Sri Lanka are not well known because of the lack of observations. One objective of this study

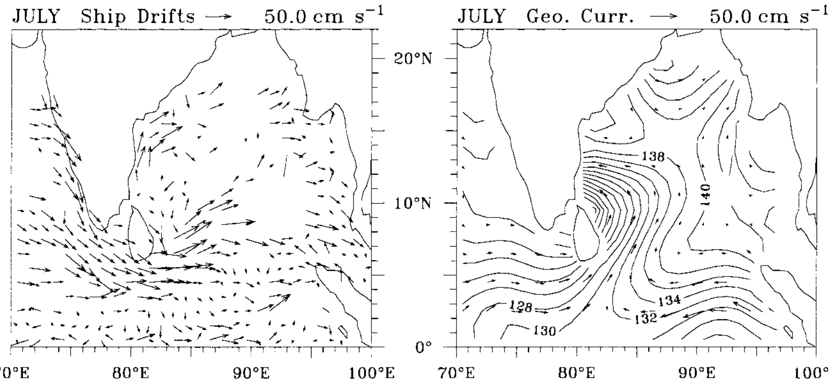

Figure 1. Climatological surface circulation around India and Sri Lanka for the month of July. (left) The climatological ship drifts [*Cutler and Swallow*, 1984]. (right) The geostrophic flow field calculated from climatological temperature [*Levitus and Boyer*, 1994] and salinity [*Levitus et al.*, 1994]. The contours in the right plot are dynamic topography (with reference to 500 m) in dynamic centimeters, and the vectors represent geostrophic currents.

is to present the geostrophic flow east of Sri Lanka making use of the expendable bathythermograph (XBT) data collected during Tropical Ocean-Global Atmosphere/World Ocean Circulation Experiment (TOGA/WOCE) and TOPEX/POSEIDON (T/P) altimeter data.

Modeling studies on the Bay of Bengal have progressed much farther than their observational counterpart [*Potemra et al.*, 1991; *Yu et al.*, 1991; *McCreary et al.*, 1993, 1996; *Shankar et al.*, 1996; *Vinayachandran et al.*, 1996]. These simulations also suggest that a part of the SMC turns northeastward and enters the Bay of Bengal. Though these studies have discussed the dynamics of the seasonal circulation in the Bay of Bengal in detail, the SMC in the vicinity of Sri Lanka was not a matter of serious concern. In a previous study, using an ocean general circulation model, VY98 found that the summer monsoon circulation around Sri Lanka consists of a large anticyclonic vortex south of Sri Lanka, a thermal dome associated with cyclonic circulation east of Sri Lanka (Sri Lanka Dome, hereafter referred to as SLD), and an anticyclonic eddy east of the SLD. In that model the intrusion of the SMC into the bay was marked by an intense northward flow between the SLD and the anticyclonic eddy to the east. It was suggested that the Rossby wave from the eastern boundary of the Bay of Bengal, which is originally due to the spring *Wyrtki* [1973] jet in the equatorial Indian Ocean, is favorable for the intrusion of the SMC into the Bay of Bengal. The exact mechanism that causes the SMC to turn around Sri Lanka, however, was not addressed.

Observations made in the eastern Indian Ocean as a part of the TOGA/WOCE program provide an opportunity to present the first estimate of the geostrophic flow east of Sri Lanka. Altimeter data measured by TOPEX/POSEIDON in the 1990s offer a horizontal view of the surface circulation. In this paper, using these two data sets and results from an ocean general circulation model (OGCM), we study the SMC around Sri Lanka in detail. Geostrophic currents calculated from the XBT data and from the altimeter data along with a description of the data are presented in section 2. Model simulation and comparisons with observations are presented in section 3. The forcing mechanism that causes the turning of the SMC around Sri Lanka is discussed in section 4. Section 5 concludes with a summary of the main results.

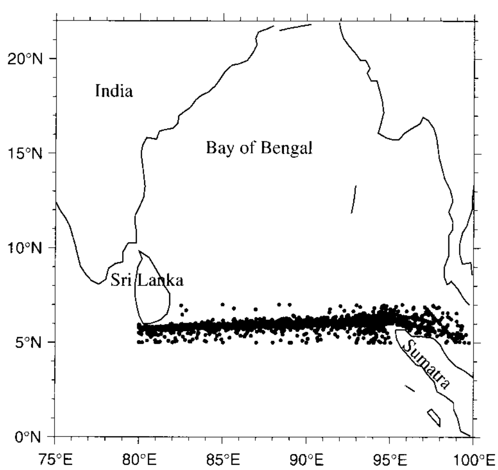

Figure 2. Map of the study area and the locations of expendable bathythermograph (XBT) measurements. Each temperature profile is represented by a dot. See Table 1 for a monthwise distribution of number of observations.

2. Geostrophic Currents

2.1. XBT Observations

As a part of the TOGA/WOCE program, temperature profiles in the upper ocean were measured intensively along major

Table 1. Monthly Distribution of Number of Temperature Profiles Along the Sri Lanka-Malaca Shipping Route During 1985–1996

Month	Profiles
January	200
February	136
March	191
April	167
May	170
June	135
July	108
August	121
September	158
October	159
November	243
December	259
Total	2047

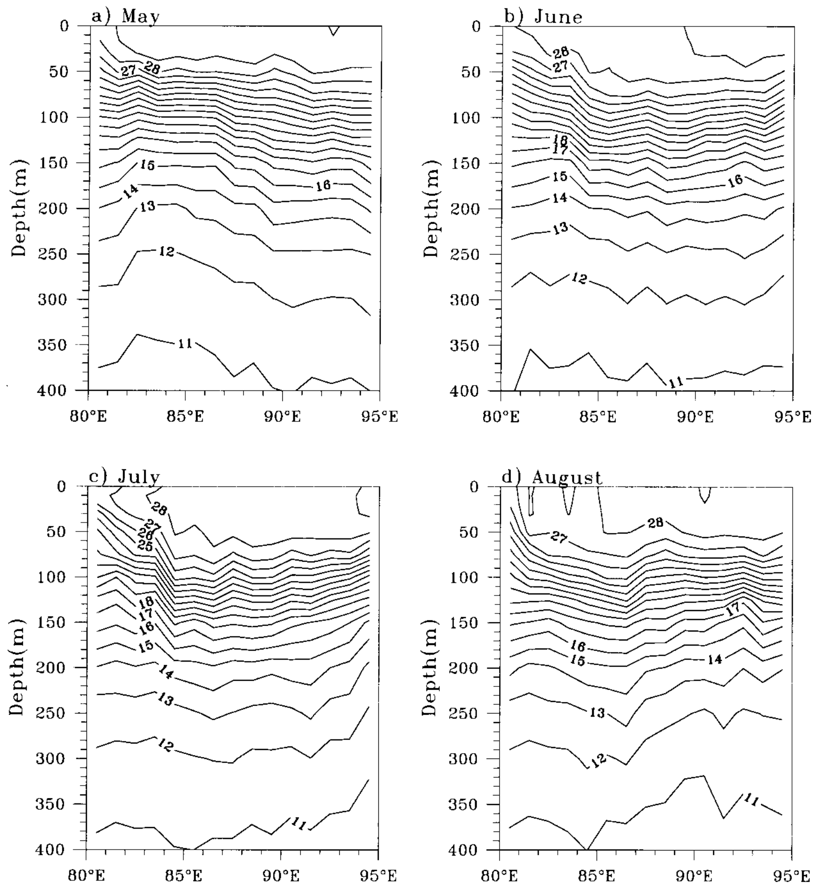

Figure 3. Vertical section of temperature along 6°N from the XBT data during (a) May, (b) June, (c) July, and (d) August. Contour interval is 1°C.

shipping routes using XBTs launched from merchant ships. Such data sets collected along the shipping route between Sri Lanka and Malaca Strait (Figure 2) and archived at the WOCE Global Subsurface Data Center (Brest, France) are used in this study. This route runs approximately along 6°N between about 80°E and 95°E. Each profile is visually checked against *Levitus and Boyer* [1994] climatology and flagged according to quality. Observations which had more than three standard deviations with climatology are not used in this analysis. The data used here consist of 2047 profiles collected during 1985–1996. The data distribution along the shipping track is shown in Figure 2, and the monthly data distribution is shown in Table 1.

A monthly climatology along 6°N spaced at intervals of 1° longitude was constructed as follows. First, the temperature data from each profile were linearly interpolated to standard depths. Then the gridded value at each depth was calculated using an objective analysis procedure described by *Kessler and McCreary* [1993]. In this procedure the gridded temperature at each standard depth is given by

$$T(x_0, y_0, t_0) = \frac{\sum_{n=1}^{N_p} T(x_n, y_n, t_n) W(x_n, y_n, t_n)}{\sum_{n=1}^{N_p} W(x_n, y_n, t_n)},$$

where N_p is the total number of observations and the weight W is given by

$$W_n(x_n, y_n, t_n) = \exp\{-[((x_n - x_0)/X)^2 + ((y_n - y_0)/Y)^2 + ((t_n - t_0)/\tau)^2]\}.$$

In the above equations, (x_0, y_0, t_0) are the coordinates of the grid point and (x_n, y_n, t_n) are the coordinates of the individual observations. Mapping scales of $X = 0.5°$ longitude, $Y = 0.5°$ latitude, and $\tau = 10$ days were used. As given by *Kessler and McCreary* [1993], the influence region was defined to be within $2\sqrt{2}$ times the mapping scale.

The monthly temperature sections for the summer monsoon months are shown in Figure 3. During May the upper level is warm at about 29°C, and the thermally mixed layer is about 30 m deep. The isotherms slope upward toward the west, and the upwelling is clear near the coast of Sri Lanka. During June and July the thermally mixed layer cools and deepens because of wind mixing, and the upwelling near the coast of Sri Lanka intensifies, bringing cooler subsurface water to the near-surface layer (Figures 3b and 3c).

Figure 4 shows geostrophic currents calculated with reference to 400 dbar, using monthly climatological salinity data from *Levitus et al.* [1994] for the summer monsoon. East of Sri Lanka, there is a strong flow into the bay during the summer which is identified here as the intrusion of the SMC into the Bay of Bengal (Figure 4). This flow is shallow, mostly confined to the upper 200 m, consistent with the observations from south of Sri Lanka [*Schott et al.*, 1994]. The current appears first during May as a broad northward flow located in the central part of the Bay of Bengal. As the season advances, this

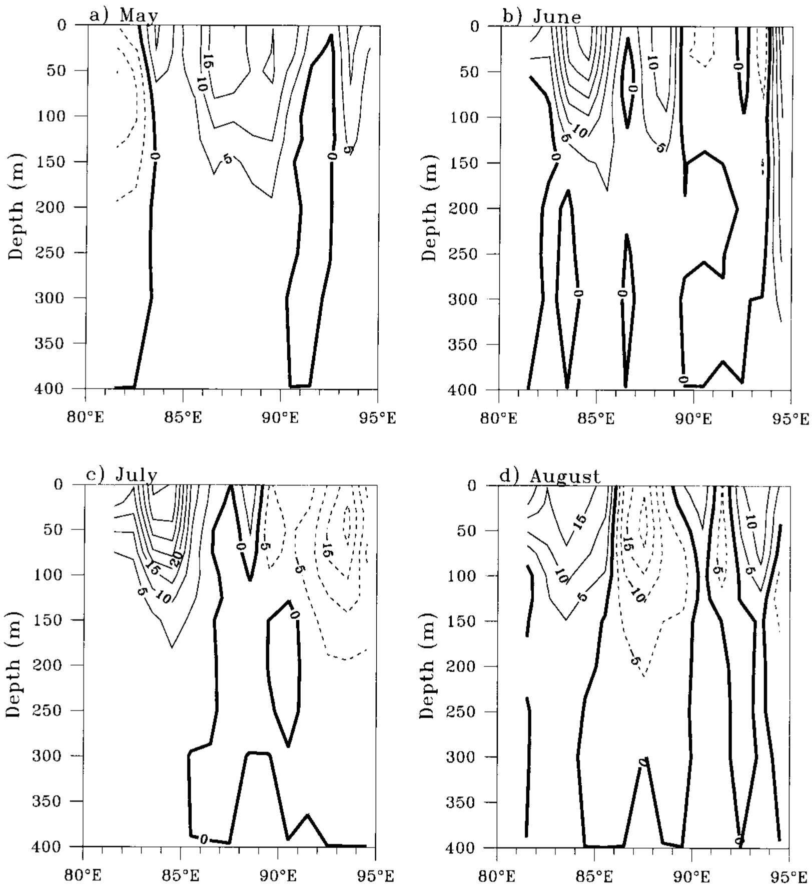

Figure 4. Vertical sections of geostrophic currents across 6°N for the months of (a) May, (b) June, (c) July, and (d) August. Geostrophic currents are calculated using XBT data and climatological salinity [*Levitus et al.*, 1994] with reference to 400 m. Contour interval is 5 cm s^{-1}. Southward flow is shown as dashed contours, and northward flow is shown as solid contours.

northward flow moves westward, narrows, and intensifies. The SMC east of Sri Lanka achieves its peak strength during July, with speeds exceeding 40 cm s^{-1}, and weakens thereafter. The transport in the upper 400 m reaches a peak value of 12 Sv during July, and most of the transport is concentrated in the upper 200 m (Figure 4). Geostrophic flow across 6°N during the rest of the year consists of alternating northward and southward bands.

2.2. TOPEX/POSEIDON Data

The altimeter data from T/P during the 1990s enable us to derive an independent estimate of the surface geostrophic currents. Further, the satellite data provide a horizontal view of the SMC. Sea level anomaly data, available at 10 day intervals with a spatial resolution of 0.5° latitude × 0.5° longitude, are used in this study. These anomalies are calculated from the mean values for the period from January 1993 to January 1996 [*Le Traon and Ogor*, 1998; *Le Traon et al.*, 1998]. We have prepared monthly mean seal level anomaly maps by combining all the maps of a given month for the period of 1993–1996. These sea level anomalies were then used to compute monthly mean geostrophic currents.

The geostrophic currents for the summer monsoon months calculated from the T/P altimetry are shown in Figure 5. The intrusion of the SMC into the Bay of Bengal is clearly seen. In fact, the T/P data suggest that the SMC as a whole turns around Sri Lanka during the summer monsoon months. As seen in the XBT data, the SMC that enters into the Bay of Bengal appears in the central part of the bay during May. This intensifies later and shifts westward but is separated distinctly from the east coast of Sri Lanka because of the SLD (VY98). After entering the Bay of Bengal, one part of the SMC recirculates as a cyclonic gyre associated with the SLD, and the rest continues to penetrate the bay reaching as far north as 20°N during August.

Figure 6 shows the comparison of meridional geostrophic currents near the surface in July across 6°N calculated from the XBT data and the T/P sea level anomalies. Both data sets show remarkable correspondence in the zonal distribution, though the SMC is stronger by about 15 cm s^{-1} in the XBT data. Nevertheless, both data sets clearly show the intrusion of the SMC into the Bay of Bengal.

3. Model Simulation

The OGCM used in this study is an Indian Ocean model based on the Geophysical Fluid Dynamics Laboratory (GFDL) modular ocean model [*Pacanowski*, 1996]. The model has realistic coastlines and topography and is bounded by latitudes 70°S and 30°N and longitudes 30°E and 115°E. There are 20 levels in the vertical, and the upper 50 m has a resolution of 10 m. Horizontal resolution is 0.5° × 0.5°; eddy viscosity and

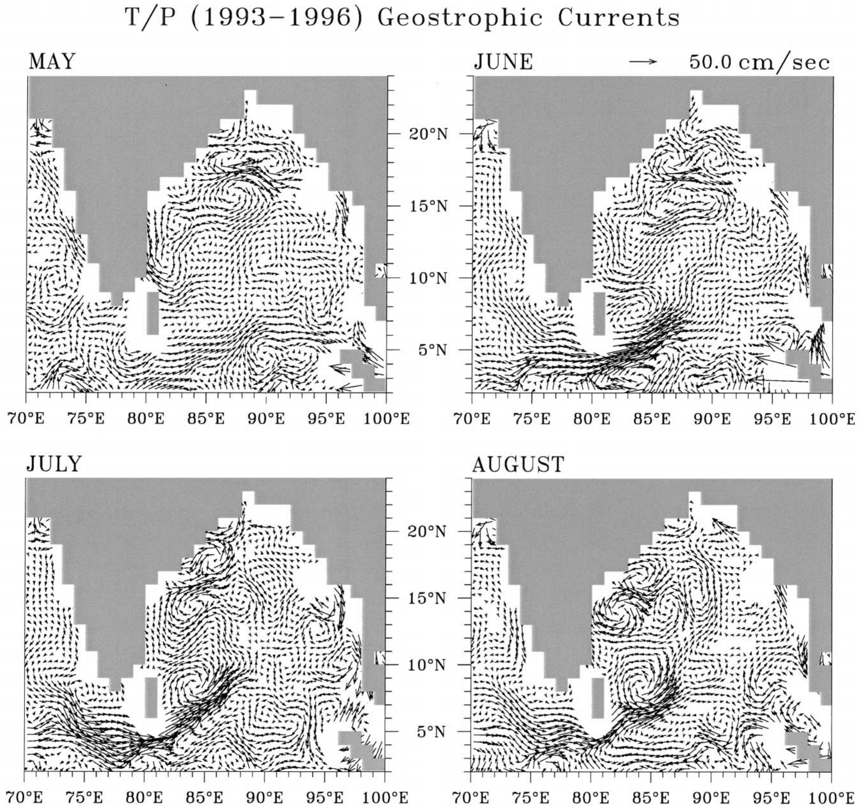

Figure 5. Geostrophic currents calculated from the sea surface height anomalies measured by the altimeter on board TOPEX/POSEIDON. The 10 day data covering the period 1993–1996 are first combined into a monthly anomaly, and then the geostrophic currents are calculated.

diffusivity are 2×10^7 cm^2 s^{-1} and 1×10^7 cm^2 s^{-1}, respectively. Vertical mixing is parameterized using a Richardson number dependent formulation [*Pacanowski and Philander*, 1981]. The model is forced by Florida State University (FSU)

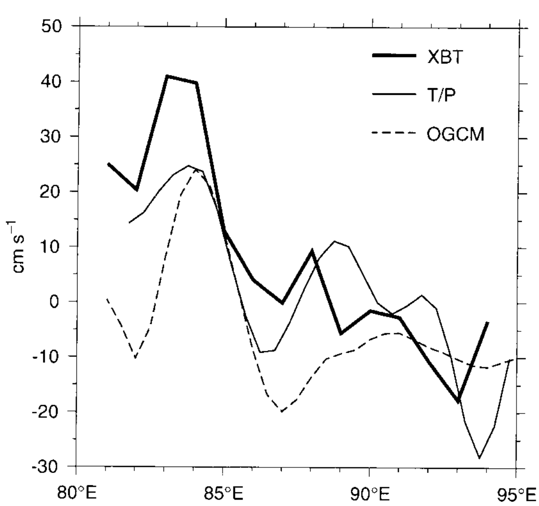

Figure 6. Comparison of the geostrophic currents calculated using XBT data (bold solid curve) and TOPEX/POSEIDON data (thin solid curve) with the meridional current from the ocean general circulation model (OGCM) (dashed line) along 6°N for the month of July. Since at the first two levels the model currents are dominated by Ekman flow, the meridional velocity at 25 m (third model level) is shown. Positive (negative) values indicate northward (southward) flow.

winds [*Legler et al.*, 1989] averaged over the period 1986–1996. A monthly climatology was constructed by averaging the data for each month for this period. To convert the pseudostress into actual wind stress, a constant drag coefficient of 0.0013 was used. South of 30°S where FSU data are not available, *Hellerman and Rosenstein* [1983] wind stress is used. The surface heat flux (Q) in the model is parameterized using the formula

$$Q = Q_c + \lambda(T - T_c),$$

where T is the model temperature at the uppermost model level and T_c is the climatological sea surface temperature. T_c is taken from *Levitus and Boyer* [1994], and Q_c is taken from *da Silva et al.* [1994]. The relaxation timescale corresponding to λ is 1/30 days. The sea surface salinity is relaxed to *Levitus et al.* [1994] climatology with the same timescale. The model is integrated for 5 years, and the results presented are for the fifth model year.

The upper level currents from the model during the summer monsoon are shown in Figure 7. The results obtained agree with a previous simulation (VY98) in which the model was forced by *Hellerman and Rosenstein* [1983] winds and *Oberhuber* [1988] heat flux. However, the anticyclonic eddy noted east of the SLD by VY98 is much weaker and located farther to the east in the present simulation (see July in Figure 7). In the present simulation the monsoon circulation around Sri Lanka during July is characterized by a cyclonic gyre east of Sri Lanka (SLD) and a large anticyclonic vortex embedded in the SMC south of Sri Lanka (Figure 7). The SMC flows eastward south of Sri Lanka and turns northeastward to flow into the Bay of

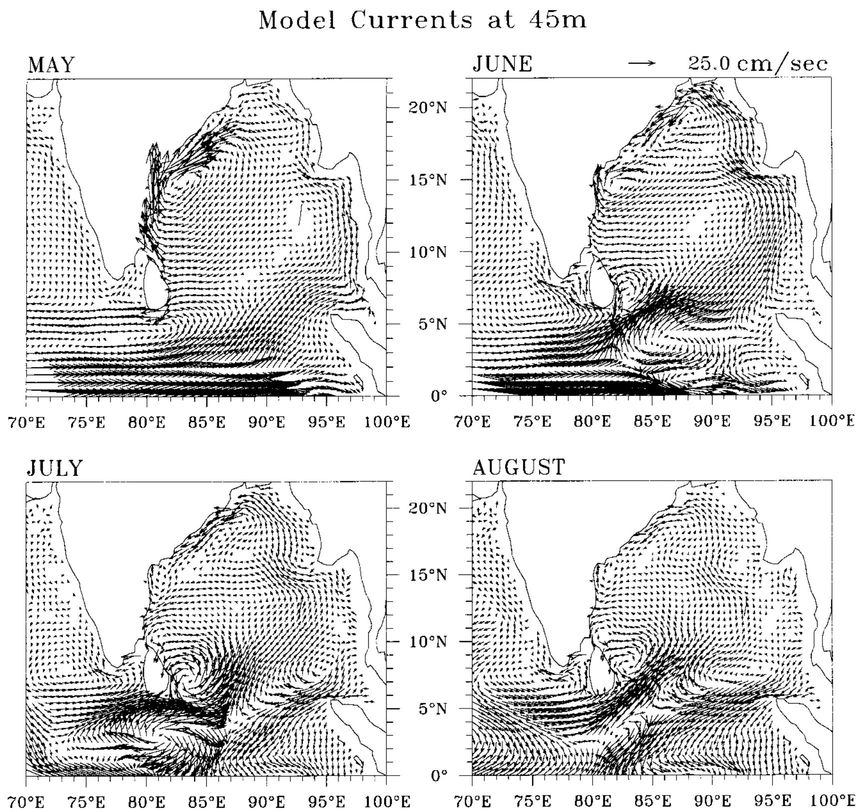

Figure 7. Current at a depth of 45 m during May, June, July, and August from the ocean circulation model described in section 3. This is a snapshot of the model on the fifteenth of the month from the fifth year of the model run.

Bengal. The initial development of the intrusion of the model SMC is closer to the eastern boundary than in the XBT and T/P data. The southwest-northeast orientation of the model current near the eastern boundary is attributed to the Rossby waves associated with the reflection of the spring *Wyrtki* [1973] jet from the eastern boundary. By June this flow pattern moves westward, so that the eastward branch of the SMC south of India intensifies. In agreement with the geostrophic currents derived from altimeter data the major part of the model SMC flows into the Bay of Bengal. We note that Rossby wave front is associated with southwestward currents on its leeward side (east of about 85°E), as seen in Figure 5.

In Figure 6 the meridional velocity across 6°N from the model is compared with the geostrophic currents calculated from XBT observations (section 2.1) and T/P data (section 2.2). All curves show a peak in speed east of Sri Lanka associated with the intrusion of the SMC into the Bay of Bengal. The speed of the model SMC is smaller than the geostrophic current calculated from XBT data but is very close to that from T/P data. It should be noted that the geostrophic currents calculated from the XBT data are biased by the use of climatological salinity. The zonal variation of the current is similar in both model and XBT observations. However, the peak near 88°E seen in the geostrophic currents is not seen in the model result.

4. Forcing Mechanisms

Modeling studies in the past have suggested two important mechanisms that drive the summer monsoon circulation in the interior of the Bay of Bengal far from the boundaries. The first one is due to the Ekman pumping by the winds over the Bay of Bengal. The winds over the Bay of Bengal are southwesterlies during summer (Figure 8), and they possess positive (cyclonic) curl in the western part of the Bay of Bengal and negative (anticyclonic) curl in the eastern part. In particular, the curl of the wind stress has large positive value around Sri Lanka. This large cyclonic curl drives a cyclonic circulation east of Sri Lanka leading to the formation of the SLD (VY98).

The second mechanism is due to the Rossby wave radiated from the eastern boundary, primarily by the reflection of the eastward spring Wyrtki jet in the equatorial Indian Ocean. During the transition between monsoons (i.e., during April–May and October–November) the westerly winds along the equatorial Indian Ocean drive intense eastward jets [*Wyrtki*, 1973]. The Kelvin wave associated with these equatorial jets propagates eastward, and on meeting the eastern boundary, one part of the energy reflects as a Rossby wave and the other propagates poleward as a coastal Kelvin wave [*Moore and Philander*, 1977]. The presence of these waves in climatological hydrographic data and numerical models has been confirmed [e.g., *Yamagata et al.*, 1996], and their implications to the circulation in the Bay of Bengal has been studied in detail [*Potemra et al.*, 1991; *Yu et al.*, 1991; *McCreary et al.*, 1993, 1996; *Kumar and Unnikrishnan*, 1995; *Shankar et al.*, 1996; *Vinayachandran et al.*, 1996].

While the first mechanism can affect the SMC locally as well as remotely through Rossby waves generated in the eastern part of the ocean, the second mechanism influences the SMC by Rossby wave radiation from the eastern boundary. VY98 noted that a Rossby wave associated with reflection of the spring Wyrtki jet is present south and east of Sri Lanka during the summer monsoon. As given by VY98, the nonlinear interaction of the Rossby wave front with the eastward current [*Greatbatch*, 1985] leads to the formation of a large anticyclonic vortex south of Sri Lanka (Figure 7c).

The depth of the 20°C isotherm (hereafter D20), which is well embedded within the thermocline (Figure 3), was chosen to examine the Rossby wave propagation along 6°N. Annual and semiannual harmonics of the anomaly of the D20 from the annual mean for the XBT data are shown in Figure 9 with bold solid lines. Near the eastern boundary the semiannual component shows a larger amplitude than the annual one. In the west the semiannual component is very weak. Where the SMC enters into the Bay, the annual harmonic has a larger contribution to the total variance. The annual phase shows a decrease toward the west near the eastern boundary and reaches a nearly steady value in the central part of the Bay of Bengal. Clear westward propagation is seen west of 85°E starting during the midsummer monsoon. However, the semiannual phase shows clear westward propagation from the eastern boundary, and the signal weakens as it propagates westward. The semiannual signal leaves the eastern boundary during May–June (October–November) matching the timing of the Wyrtki jets. A straight line fit to the phase of either annual or semiannual harmonic component shows that the signal takes 98 days to propagate across the bay at 6°N, giving a phase speed of about 20.8 cm s^{-1} which is in close agreement with Rossby wave theory. Phase speed of linear nondispersive Rossby wave at 6°N is given by 20.2 cm s^{-1} if we assume a reduced gravity model in which the mixed layer depth is 50 m, mixed layer temperature is 28°C, and the temperature below is 14°C. This signal corresponds primarily to a second baroclinic mode Rossby wave [*Shankar et al.*, 1996].

In order to elucidate the reflection at the eastern boundary as well as the Ekman pumping within the bay that causes the observed variation of the D20, we adopt a simple forced Rossby wave model. Assuming that the variation of the thermocline is due to the Ekman pumping and long Rossby wave propagation, the isotherm displacement (h) is given by [*Meyers*, 1979]

$$h_t + ch_x = W,$$

where W is the Ekman pumping velocity and c is the nondispersive phase speed of the long Rossby waves, t is the time, and x is the distance from the eastern boundary. A value of 21 cm s^{-1} is used for the phase speed, and the Ekman pumping velocity along 6°N is calculated from the FSU winds (section 3). As given by *Masumoto and Meyers* [1998], two cases are studied: In the first the variations at the eastern boundary are fixed to zero so that the variation of the D20 in the model is caused entirely by the Ekman pumping. In the second case the values of D20 variation from the XBT data near the eastern boundary are added so that the effect of the Rossby wave radiation from the eastern boundary is also included. The results, decomposed into annual and semiannual components, are also shown in Figure 9.

The phase of the semiannual signal is well reproduced by the case which includes the eastern boundary signal (Figure 9, thin solid curve). In the absence of the Rossby wave radiation from the eastern boundary (dashed curve) the phase does not show

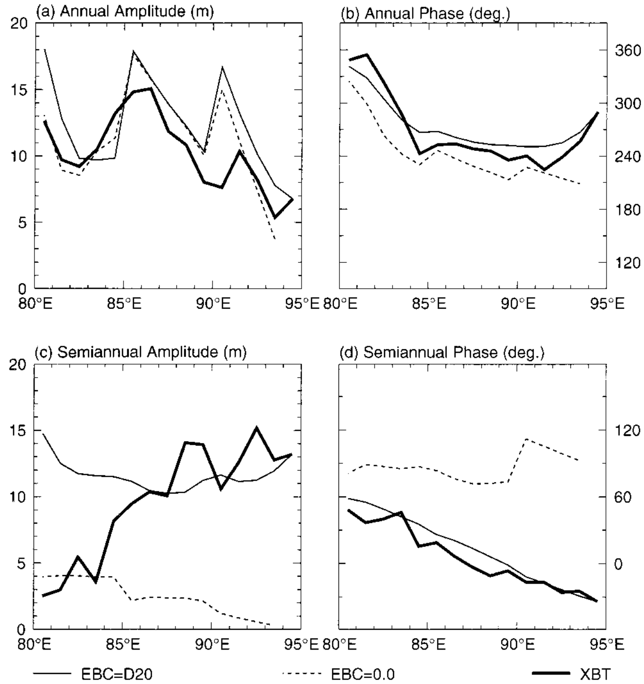

Figure 9. (a) Annual amplitude, (b) annual phase, (c) semiannual amplitude, and (d) semiannual phase of the depth of the 20°C isotherm. The units are meters for amplitude and degrees for phase. Bold solid curve corresponds to the value calculated from XBT observations. Thin solid curve corresponds to the value calculated from the result of the simple model (section 4) imposing the depth of 20°C from the XBT data as a boundary condition near the eastern boundary, and the dashed curve corresponds to the simple model calculation with zero value for the anomaly of the depth of the 20°C isotherm at the eastern boundary.

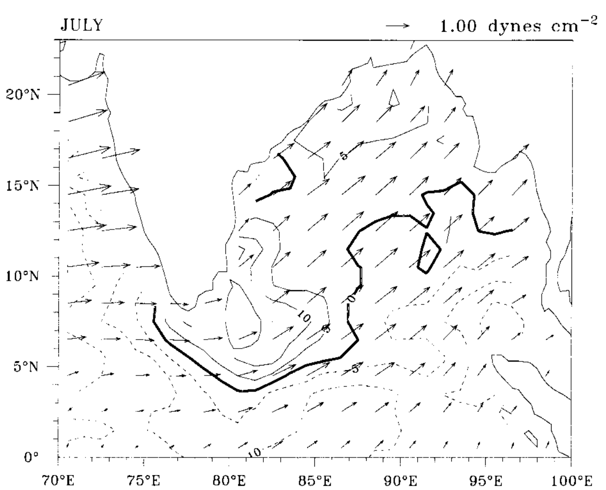

Figure 8. Mean monthly wind stress during July for the period 1986–1996 from Florida State University pseudostress data. A drag coefficient of 0.0013 is used to convert the pseudostress into wind stress. Vectors represent wind stress plotted at every alternate grid point, and the contours represent the curl of the wind stress in units of 10^{-9} dynes cm^{-3}. A region of large positive (cyclonic) vorticity develops east of Sri Lanka during the southwest monsoon (May–September).

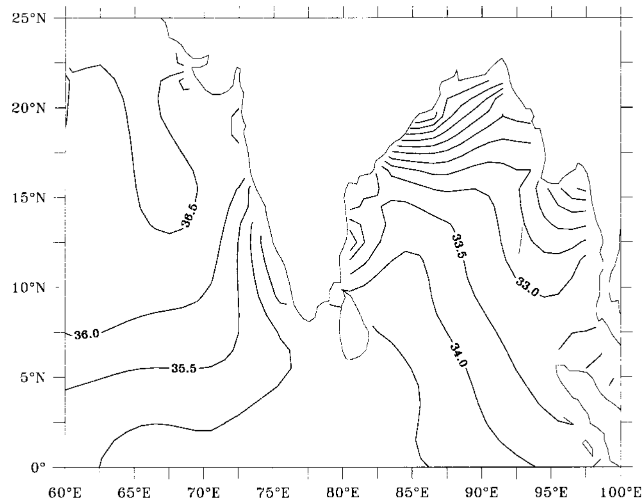

Figure 10. Horizontal distribution of the salinity at the sea surface from the climatological data set [*Levitus et al.*, 1994]. Contour interval is 0.5 psu. Note the flow of high-salinity water from the Arabian Sea into the Bay of Bengal along the path of the Southwest Monsoon Current.

clear westward propagation; clearly, the semiannual signal originates from the eastern boundary. The observed amplitude which has a large value in the eastern part of the Bay of Bengal (Figure 9c) also suggests forcing at the eastern boundary. The slight westward increase in semiannual amplitude in both experiments is due to the lack of any damping in the model together with the weak forcing by the wind stress curl over the Bay of Bengal. The observed decrease in the amplitude toward the west suggests that the semiannual signal weakens significantly as it propagates westward.

As for the annual signal, inclusion of the eastern boundary signal does not show significant improvement in either amplitude or phase. This suggests that primarily the Ekman pumping within the Bay of Bengal causes the annual variation.

Forcing from the equatorial Indian Ocean has semiannual periodicity, and the winds over the Bay of Bengal are predominantly annual. The amplitudes of D20 variations shown in Figure 9 suggest that both Ekman pumping in the Bay of Bengal and Rossby wave radiation from the eastern boundary contribute to the generation of the Rossby wave which drives the SMC toward southeast of Sri Lanka. This is in contrast with the formation of northeastward SMC in the Bay of Bengal in a numerical experiment by *Yu et al.* [1991] in which the forcing was applied only in the equatorial Indian Ocean. In May the XBT data show that east of Sri Lanka the branch of SMC that enters the Bay of Bengal first develops in the central bay and then moves westward (Figure 4). T/P data also show the development of the southwest-northeast oriented flow before the full development of the eastward SMC south of Sri Lanka (compare May and June in Figure 5). OGCM results (section 3) clearly show the Rossby wave signal during May. These features suggest that the forcing by the spring Wyrtki jet is responsible for the initial intrusion of the SMC into the Bay of Bengal.

5. Summary

During the summer monsoon the SMC flows eastward/southeastward in the Arabian Sea and eastward south of India and Sri Lanka. Using XBT data collected along the Sri Lanka-Malaca Strait section during TOGA/WOCE, altimeter data from TOPEX/POSEIDON, and results from an OGCM, we have shown that the major part of the SMC curves around Sri Lanka and flows into the Bay of Bengal. East of Sri Lanka the SMC is about 300 km wide and about 200 m deep. Surface geostrophic speed of the current is in the range of 25–40 cm s^{-1}, and the seasonal mean (May–September) transport is 10 Sv. Zonal profile of the meridional velocity is similar among the three data sets. However, the speed of the SMC is the largest in XBT observations. The region east of Sri Lanka is forced by the Ekman pumping because of strong monsoonal winds as well as the Rossby wave radiation from the eastern boundary. We note that both winds over the Bay of Bengal and the spring Wyrtki jet in the equatorial Indian Ocean are responsible for the SMC east of Sri Lanka. The initial development of the SMC is mainly attributed to the Rossby wave reflection by the spring Wyrtki jet.

The SMC has an important role in the salt balance of the Bay of Bengal. From their numerical model experiment, VY98 suggested that the SMC serves as an open ocean link that connects the Arabian Sea and the Bay of Bengal. Observations and model results presented here confirm their finding. Figure 10 shows that the SMC brings high-salinity water from the Arabian Sea into the Bay of Bengal.

It should be noted that our transport estimate is biased by the lack of simultaneous salinity measurements. Recent observations show low-salinity water along the coast of Sri Lanka [*Schott et al.*, 1994] which is not resolved by climatological data sets. Therefore our estimate of the transport should be considered as preliminary. Future observational programs should aim at resolving this issue. They could also help to quantify the role of SMC on the freshwater (salt) balance of the Bay of Bengal. Considering that the monsoon is associated with large variability, the SMC must be influenced by large intraseasonal and interannual variations. This issue is deferred for a future study.

Acknowledgments. XBT data collected by *Kashimasan Maru*, as a part of the Japanese Experiment on Asian Monsoon (JEXAM), supported by Science and Technology Agency triggered off this study. Thanks to Marie-Claire Fabri (IFREMER/SISMER, Brest, France) for providing the XBT data and P. Y. Le Traon for providing the TOPEX/POSEIDON data. The altimeter products have been produced by the CLS Space Oceanography Division as a part of the Environment and Climate AGORA EC project (ENV4-CT9560113). We thank Takashi Kagimoto for many useful discussions and R. Pacanowski for giving us the MOM2 code. FERRET (NOAA/PMEL) assisted in the data analysis and graphics.

References

Cutler, A. N., and J. C. Swallow, Surface currents of the Indian Ocean (to 25°S, 100°E): Compiled from historical data archived by the Meteorological Office, Bracknel, UK, *Rep. 187*, 8 pp., 36 charts, Inst. of Oceanogr. Sci., Wormley, England, 1984.

da Silva, A. M., C. C. Young, and S. Levitus, *Atlas of Surface Marine Data 1994*, vol. 3, *Anomalies of Heat and Momentum Fluxes*, *NOAA Atlas NESDIS* vol. 8, 413 pp., U.S. Gov. Print. Off., Washington, D. C., 1994.

Greatbatch, R. J., Kelvin wave fronts, Rossby solitary waves and nonlinear spin-up of the equatorial oceans, *J. Geophys. Res.*, *90*, 9097–9107, 1985.

Hastenrath, S., and L. Greischar, The monsoonal current regimes of the tropical Indian Ocean: Observed surface flow fields and their geostrophic and wind-driven components, *J. Geophys. Res.*, *96*, 12,619–12,633, 1991.

Hellerman, S., and M. Rosenstein, Normal monthly wind stress over the world ocean with error estimates, *J. Phys. Oceanogr.*, *13*, 1093–1104, 1983.

Kessler, W. S., and J. P. McCreary, The annual wind-driven Rossby wave in the subthermocline equatorial Pacific, *J. Phys. Oceanogr.*, *23*, 1192–1207, 1993.

Kumar, S. P., and A. S. Unnikrishnan, Seasonal cycle of temperature and associated wave phenomena in the upper layers of the Bay of Bengal, *J. Geophys. Res.*, *100*, 13,585–13,593, 1995.

Legler, D. M., I. M. Navon, and J. J. O'Brien, Objective analysis of pseudo-stress over the Indian Ocean using a direct-minimization approach, *Mon. Weather Rev.*, *117*, 709–720, 1989.

Le Traon, P. Y., and F. Ogor, ERS-1/2 orbit improvement using TOPEX/POSEIDON: The 2 cm challenge, *J. Geophys. Res.*, *103*, 8045–8057, 1998.

Le Traon, P. Y., F. Nadal, and D. Ducet, An improved mapping method for multisatellite altimeter data, *J. Atmos. Oceanic Technol.*, *15*, 522–534, 1988.

Levitus, S., and T. P. Boyer, *World Ocean Atlas 1994*, vol. 4, *Temperature*, *NOAA Atlas NESDIS*, vol. 4, 117 pp., U.S. Gov. Print. Off., Washington, D. C., 1994.

Levitus, S., R. Burgett, and T. P. Boyer, *World Ocean Atlas 1994*, vol. 5, *Salinity*, *NOAA Atlas NESDIS*, vol. 3, 99 pp., U.S. Gov. Print. Off., Washington, D. C., 1994.

Masumoto, Y., and G. Meyers, Forced Rossby waves in the Southern tropical Indian Ocean, *J. Geophys. Res.*, *103*, 27,589–27,602, 1998.

McCreary, J. P., P. K. Kundu, and R. L. Molinari, A numerical investigation of dynamics, thermodynamics and mixed-layer processes in the Indian Ocean, *Prog. Oceanogr.*, *31*, 181–244, 1993.

McCreary, J. P., W. Han, D. Shankar, and S. R. Shetye, Dynamics of the east India coastal current, 2, Numerical solutions, *J. Geophys. Res.*, *101*, 13,993–14,010, 1996.

Meyers, G., On the annual Rossby wave in the tropical North Pacific Ocean, *J. Phys. Oceanogr.*, *9*, 663–674, 1979.

Moore, D. W., and S. G. H. Philander, Modeling of the tropical oceanic circulation, in *The Sea: Ideas and Observations in the Study of the Sea*, vol. 6, edited by E. D. Goldberg et al., pp. 319–369, Wiley Interscience, New York, 1977.

Oberhuber, J. M., An atlas based on "COADS" data set, *Rep. 15*, Max-Planck-Inst. für Meteorol., Hamburg, Germany, 1988.

Pacanowski, R., MOM2 Version 2.0 (Beta): Documentation, user's guide and reference manual, *GFDL Ocean Tech. Rep. 3.2*, 329 pp., Geophys. Fluid Dyn. Lab., Princeton, N. J., 1996.

Pacanowski, R. C., and S. G. H. Philander, Parameterization of vertical mixing in numerical models of the tropical ocean, *J. Phys. Oceanogr.*, *11*, 1442–1451, 1981.

Potemra, J. T., M. E. Luther, and J. J. O'Brien, The seasonal circulation of the upper ocean in the Bay of Bengal, *J. Geophys. Res.*, *96*, 12,667–12,683, 1991.

Schott, F., Monsoon response of the Somali Current and the associated upwelling, *Prog. Oceanogr.*, *12*, 1343–1357, 1983.

Schott, F., J. Reppin, J. Fischer, and D. Quadfasel, Currents and transports of the monsoon current south of Sri Lanka, *J. Geophys. Res.*, *99*, 25,127–25,141, 1994.

Shankar, D., J. P. McCreary, W. Han, and S. R. Shetye, Dynamics of the East India Coastal Current, 1, Analytic solutions forced by interior Ekman pumping and local alongshore winds, *J. Geophys. Res.*, *101*, 13,975–13,991, 1996.

Shetye, S. R., A. D. Gouveia, S. S. C. Shenoi, G. S. Michael, D. Sundar, A. M. Almeida, and K. Santanam, The coastal current off western India during the northeast monsoon, *Deep Sea Res.*, *38*, 1517–1529, 1991.

Shetye, S. R., A. D. Gouveia, D. Shankar, S. S. C. Shenoi, P. N. Vinayachandran, D. Sundar, G. S. Michael, and G. Nampoothiri, Hydrography and circulation in the western Bay of Bengal during the northeast monsoon, *J. Geophys. Res.*, *101*, 14,011–14,025, 1996.

Vinayachandran, P. N., and S. R. Shetye, The warm pool in the Indian Ocean, *Proc. Indian Acad. Sci. Earth Planet. Sci.*, *100*, 165–175, 1991.

Vinayachandran, P. N., and T. Yamagata, Monsoon response of the sea around Sri Lanka: Generation of thermal domes and anticyclonic vortices, *J. Phys. Oceanogr.*, *28*, 1946–1960, 1998.

Vinayachandran, P. N., S. R. Shetye, D. Sengupta, and S. Gadgil, Forcing mechanisms of the Bay of Bengal circulation, *Current Sci.*, *71*, 753–763, 1996.

Wyrtki, K., An equatorial jet in the Indian Ocean, *Science*, *181*, 262–264, 1973.

Yamagata, T., K. Mizuno, and Y. Masumoto, Seasonal variations in the equatorial Indian Ocean and their impact on the Lombok throughflow, *J. Geophys. Res.*, *101*, 12,465–12,473, 1996.

Yu, L., J. J. O'Brien, and J. Yang, On the remote forcing of the circulation in the Bay of Bengal, *J. Geophys. Res.*, *96*, 20,449–20,454, 1991.

Y. Masumoto and T. Yamagata, Department of Earth and Planetary Physics, Graduate School of Science, University of Tokyo, Tokyo 113-0033, Japan. (e-mail: masumoto@ocean.geoph.s.u-tokyo.ac.jp; yamagata@geoph.s.u-tokyo.ac.jp)

T. Mikawa, Climate Prediction Division, Japan Meteorological Agency, 1-3-4 Otemachi, Tokyo 100-0004, Japan. (e-mail: mikawa@umi.hq.kishou.go.jp)

P. N. Vinayachandran, Institute for Global Change Research, Frontier Research System for Global Change, Seavans-N, 1-2-1 Shibaura, Tokyo 105-6795, Japan. (e-mail: vinay@frontier.esto.or.jp)

(Received July 20, 1998; revised December 23, 1998; accepted January 28, 1999.)